

## Magnetic anomaly of the Jõhvi iron ore, northeastern Estonia, controlled by subvertical remanent magnetization

Jüri Plado<sup>a</sup>, Kalle Kiik<sup>a</sup>, Jarkko Jokinen<sup>b</sup> and Alvar Soesoo<sup>a</sup>

<sup>a</sup> Department of Geology, University of Tartu, Ravila 14A, 50411 Tartu, Estonia; [juri.plado@ut.ee](mailto:juri.plado@ut.ee)

<sup>b</sup> Loop and Line Oy, Tumpppi 6A, 02400 Kirkkonummi, Finland

Received 29 June 2020, accepted 28 August 2020, available online 11 November 2020

**Abstract.** The Jõhvi magnetic anomaly is situated within the Jõhvi structural zone that is part of the Bergslagen–Livonia microcontinent. Drilling in the 1930s and 1960s has revealed a complex of magnetite ore alternating with granites, pegmatites and gneisses. The study presents the results of ground magnetic mapping, measurements of drill core (Jõhvi I and II) petrophysical properties (density, magnetic susceptibility, intensity and inclination of the natural remanent magnetization), modelling of the anomalous magnetic field in the Jõhvi area and frequency domain electromagnetic (FrEM) measurements. The magnetic anomaly is composed of three major peaks named western, eastern and northern anomalies. The maximum amplitude of the western total field anomaly is 19 290 nT, of the eastern anomaly 15 880 nT and of the northern anomaly 8080 nT. The 3-dimensional model along five profiles extends from the basement surface to a depth of 1000 m. The direction of strong remanent magnetization coincides with the dip of the iron ore formation. The strong remanence hints at the significant presence of small (<1 µm) magnetite grains in the Jõhvi ore, which needs future (magneto)mineralogical investigation. Results of the FrEM coincide with our earlier knowledge of the electrical resistivity of the crystalline basement and Phanerozoic cover. The method, however, did not provide much information on the ores due to the screening effect of the ~200 m thick pile of low-resistivity Cambrian and Ediacaran clays and sandstones on top of the Palaeoproterozoic basement.

**Key words:** magnetic field, magnetic susceptibility, natural remanent magnetization, geophysical modelling, frequency-domain electromagnetic method, Jõhvi, Estonia.

### INTRODUCTION

The Precambrian geology of platform areas is mainly based on geological drilling and geophysical data. Among geophysical methods, magnetic survey, which is relatively fast and simple to apply, and detail-rich compared to other methods, has played an especially important role in basement studies because rocks commonly retain magnetism that originates from the time of their formation. In a regional scale magnetic anomaly data thus provide a unique opportunity to infer geological processes not readily observed through other geophysical quantities (e.g., Nehlig et al. 2002; Nasuti et al. 2015). Usually, the Phanerozoic sedimentary cover has low magnetization and the signal mirrors the structure of the deeper crystalline basement. Regional aeromagnetic mapping campaigns of Estonia in 1987–1991 (Metlitskaya & Papko 1992), together with petrographical, geochemical and gravimetric data, have

resulted in the latest published revisions (Koistinen 1994; Koppelmaa 2002; Soesoo et al. 2020) of the Palaeoproterozoic crystalline basement.

The prominent, up to 20 000 nT (high fraction of a recent geomagnetic field of ~52 300 nT) Jõhvi magnetic anomaly (Fig. 1A) was, however, found before the aeromagnetic ‘era’ started in the former USSR in the 1950s (Rundqvist & Mitrofanov 1993). The discovery was made by the department of military topography during the mapping of magnetic declination and qualified in the course of the magnetic mapping in 1935–1937. Differt (1936) and Linholm (1937) suggested that the anomaly is produced by a capacious ( $6 \times 10^9 \text{ m}^3$ ) body of iron ore. Immediately, a private company ‘Magna, Ltd.’ was established and started coring at the anomaly’s highest location, already in 1937–1939 (Linari 1940). The drilling activity resulted in two vertical cores, Jõhvi I and II with depths of 505.0 and 721.5 m, respectively (Fig. 1B). Magnetite was identified as the main ore mineral and

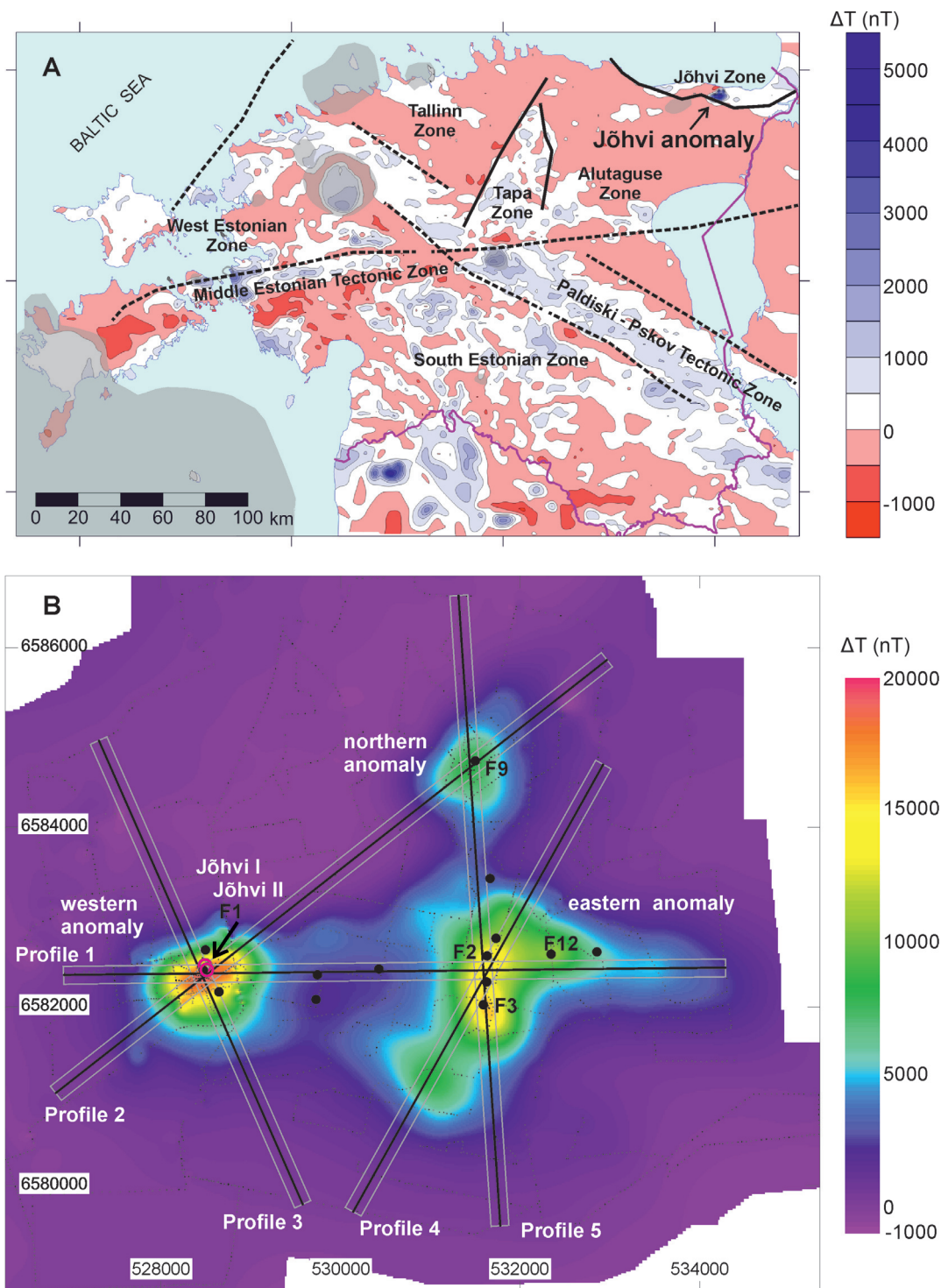


**Fig. 1. A,** structural features and metamorphic complexes of the Precambrian basement compared to aeromagnetic anomaly maps. Grey areas represent anorogenic complexes of rapakivi and related granites; the rest are Svecofennian metamorphic and plutonic rocks. Geological data are after Puura et al. (1997) and Bogdanova et al. (2015). The aeromagnetic overview map is by the Geological Survey of Estonia. The Jõhvi anomaly within the Jõhvi Zone in NE Estonia is indicated. **B,** total magnetic intensity anomaly map of the Jõhvi anomaly based on the year 2019 measurements. Shown are the profiles for magnetic modelling and location of drill holes (black dots). Drilling was performed in the late 1930s (Jõhvi I and II in the centre of the western anomaly) and 1960s (rest of the holes marked). Physical properties of the Jõhvi series cores only were measured during the present study, whereas the rest has perished. Small black marks show the individual measurements. Coordinates are in the UTM zone 35N.

source of the anomaly with small quantities of pyrite and pyrrhotite present (Vagapova-Kadyrova 1948). Sporadic occurrence of chalcopyrite was reported as well.

The anomaly was drilled again in 1967–1968 during the regional geological and geophysical campaign (Erisalu et al. 1969). Drilling into the anomaly resulted in five F-series cores (Fig. 1B), which intersected magnetite-rich quartzites (Mt-quartzites). Unfortunately, all of these cores have perished in the 1990s.

The Jõhvi anomaly is situated within the Jõhvi structural/geological zone (Fig. 1A) that is likely a part of a magmatic-volcanic-sedimentary Bergslagen–Livonia ‘microcontinent’ (Bogdanova et al. 2015). The zone consists of various types (pyroxene, quartz-feldspar, biotite-plagioclase, amphibole and garnet-cordierite) of gneisses, and Mt-quartzites at the location of the Jõhvi magnetic anomaly. Widespread migmatization has resulted in the formation of plagioclase and potassium-feldspar porphyroblasts, occasionally leucosomes and small granitoid veins, and bodies with charnockitic and enderbitic compositions (Soesoo et al. 2004, 2006). Generally, these rocks have formed under the conditions of granulite facies metamorphism (Koistinen et al. 1996). Two concepts of ore genesis have been proposed for Jõhvi ore. These include (i) metasomatism (Linari 1940; Vagapova-Kadyrova 1948; Tikhomirov 1966) and (ii) metamorphism of original volcanogenic-sedimentary rocks (Puura & Kuuspalu 1966; Erisalu et al. 1969).

Here we report results of recent (2019) ground magnetic mapping, petrophysical properties of the Jõhvi I and II drill cores, geological model based on a magnetic map and frequency domain electromagnetic (FrEM) experiment. These studies were carried out to specify the dimensions of source bodies causing the Jõhvi anomaly and to link the anomalies with rock magnetic properties. The ground magnetic mapping data were used by the Geological Survey of Estonia to locate and sight the new (2019–2020) drill holes (not reported here) into the rocks causing the Jõhvi magnetic anomaly.

## METHODS

Density ( $\rho$ ; kg/m<sup>3</sup>), magnetic susceptibility ( $\chi$ ; SI), the intensity and direction of natural remanent magnetization (NRM) ( $J_r$ ; A/m) were measured on 100 samples from the Jõhvi I and II drill cores. About 60% of the samples (cubes with sides of 20–22 mm were cut from the cores) represent Mt-quartzites, the rest are surrounding host rocks. Archimedes’ principle for density was used. Agico’s magnetic susceptibility meter KLY5 and spinner magnetometer JR-6A were used to measure  $\chi$  and  $J_r$ , respectively.

Ground magnetic measurements in the Jõhvi area were carried out in 2019 using the G-856AX proton precession

magnetometer by Geometrics, Inc. A hand-held GPS device (GARMIN eTREX20) was used to attain measurement location data. Individual measurements of the total magnetic field intensity were performed every 25–100 m along roads, division lines between forest compartments, occasionally in the forest, and tied with location coordinates. An area of ~50 km<sup>2</sup> was covered with 2897 measurements. The ground survey readings were corrected against the Nurmijärvi (Finland) magnetic observatory readings. The magnitudes of diurnal variations were <100 nT.

Successive direct magnetic modelling was performed with software Potent v.4.16.07 (Geophysical Software Solutions Pty. Ltd.). Magnetic susceptibility of the background was set to  $27 \times 10^{-3}$  SI corresponding to the average of Jõhvi Zone migmatites (Puura et al. 1983). The International Geomagnetic Reference Field parameters (field intensity  $F = 52\,254$  nT, an inclination  $I = 73.2^\circ$  and declination  $D = 9.8^\circ$ ) for the Jõhvi area in 2019 were used for an inducing field. A plane surface regional field of 52 172.7 nT was extracted from the field measurements to get the residual (anomaly) field (Fig. 1B). The regional field was estimated by averaging tens of field values from outside the anomalous area. Direct modelling was performed along five profiles with locations shown in Fig. 1B. The model is 3-dimensional, consisting of five vertical elliptic cylinders that extend from basement top surface (230–255 m; estimated from drilling data in locations given in Fig. 1B) to a depth of 1000 m. By changing the horizontal position and size of ellipses and magnetic properties of cylinders, we tried to match the model curves to fit the observed residual field by trial-and-error. The final adjustments were made automatically by Potent toolbox ‘Iteration’. Iteration compares the response of the model with anomalous values in all the originally measured locations and changes the selected, by interpreter, model parameters to obtain the best fit between the observed and calculated values at every measured location simultaneously.

Electromagnetic conductivity measurement was performed in the summer of 2019. The used FrEM method consists of a large transmitter antenna that generates a harmonically oscillating magnetic field at several frequencies and a mobile receiver with three orthogonal measuring coils. A total of 41 multi-frequency (from 116 to 9921 Hz) soundings were made on roads and paths across the study area in the vicinity and top of the westernmost anomaly (Fig. 1B). The measurement aimed to test the applicability of the system to obtain bedding information on the iron formation. A description of the measurement method can be found in the article by Aittoniemi et al. (1987) with the difference that the FrEM method uses a fixed large transmitter.

## RESULTS

The Jõhvi I drill core contains mostly two rock types – granites and granitic pegmatite, and magnetite-rich quartzites, whereas Jõhvi II consists of different gneisses in addition to pegmatite and Mt-quartzites (Puura & Kuuspalu 1966). The physical properties of Mt-quartzites differ significantly from those of other rock types (Fig. 2, Table 1). Compared to others, Mt-quartzite is characterized by high magnetization seen in high values of  $\chi$  and intensity of  $J_r$ , and  $\rho$ . They also exhibit a significantly high Koenigsberger ratio ( $Q$ ). Gneisses in the Jõhvi II core are denser and more magnetic than granitic pegmatites.

The direction of  $J_r$  is given by  $D$  and  $I$ . As the Jõhvi drill holes were made unoriented and the cores have rolled freely during the drilling process,  $D$  does not have any meaning and is not illustrated. Assuming, but not ensuring, the drillings were vertical,  $I$  shows a slight tendency towards vertical remanence [of all the rock types 29% have subhorizontal (0–30°), 32% intermediate (30–60°) and 39% subvertical (60–90°) inclination]. Within the family of Mt-quartzites, upwards directed remanence prevails (27% of measurements show inclination between –90° and –60°, whereas only 8% incline between +90° and +60°). These results differ from the modelling results below, which indicate strong and positive (directed downwards)  $J_r$ . There is no biunique explanation for the difference, but we cannot certify that all the measured samples are in the right position, i.e. the upper and lower ends of core pieces have not changed their positions during the 80 years of post-dating the drilling activities. Also, a post-drilling viscous component and/or application of strong external magnetic fields able to affect the properties of remanence cannot be excluded.

The magnetic anomaly in Jõhvi is composed of three major peaks hereafter named western, eastern and northern anomalies (Fig. 1B) according to cardinal directions relative to the centre of the complex of Jõhvi anomalies. The maximum amplitude of the **western** total field anomaly is 19 290 nT (Fig. 3A–C). The longer axis of the anomaly is directed WSW–ENE. The width of the anomaly at its half amplitude ( $2x_{1/2}$ ) in this direction is 980 m, while it is 700 m along the shorter axis (here and below  $2x_{1/2}$  represents an empirical depth estimation of the centre of theoretical magnetic dipole producing the anomaly; Peters 1949). To simulate the anomaly, an elliptic cylinder (denoted W) was created with horizontal dimensions provided in Fig. 4. The cylinder has  $\chi$  of  $350 \times 10^{-3}$  SI and  $J_r$  of 99.5 A/m resulting in the  $Q$ -ratio of 7.1. The declination and inclination were set to 173.6° and 78.6°, respectively.

The **northern** anomaly is almost symmetrical in a plan view, being slightly elongated in the NNE direction (Fig. 1B). The amplitude of the anomaly is less (max

equals to 8080 nT) than that of the western anomaly, resulting in lower  $\chi$  ( $200 \times 10^{-3}$  SI),  $J_r$  (23.3 A/m) and  $Q$  (2.9) of the model (elliptic cylinder N, Figs 3B, E, 4). Depending on the direction, the value of  $2x_{1/2}$  varies between 930 and 970 m. The declination and inclination of  $J_r$  were iterated to 345.8° and 64.0°, respectively.

Compared to the western and northern anomalies, the **eastern** anomaly has a complicated plan view where the main ellipse-shaped SSW–NNE-elongated anomaly (Fig. 1B) is ‘tailed’ with anomalous values from the east and SSW. Pobul (1961) suggested that the faulting of tectonic origin and shifts of blocks in response to each other cause the complexity. Along the longer axis (without considering the ‘tails’) the value of  $2x_{1/2}$  is ~1300 m, and ~700 m perpendicular to that. The maximum amplitude of the anomaly is 15 880 nT. To simulate the measured field, three elliptic cylinders were created, labelled E1, E2 and E3 (Figs 3A, D, E, 4). Their  $\chi$  ranges from  $200 \times 10^{-3}$  (E2 and E3) to  $250 \times 10^{-3}$  (E1) SI. At given intensities of NRM (E1: 37.5 A/m; E2: 19.9 A/m; E3: 23.5 A/m), the cylinders have  $Q$ -ratios of 3.8, 2.6 and 3.0, respectively. The declinations and inclinations are given numerically in Fig. 3 and illustrated by a stereoplot in Fig. 3F.

The most significant misfit between the measured data and calculated curve exists between the western and eastern anomalies (Fig. 3A), and eastern and northern anomalies (Fig. 3E). These are the regions where the measured anomalous field is stronger than the response curves by our geometrical models that are located aside. Even the previous drillings into these regions have not discovered any significant iron ore occurrences; some minor accessory presence of magnetite has been reported (Erisalu et al. 1969). Also, one can speculate on some deeper presence of magnetite-bearing rocks (drillings have stopped within a few tens of metres into the basement).

## DISCUSSION

The magnetic anomaly of a geological source structure is proportional to the contrast in magnetization  $J$  (A/m) to surrounding rocks, a function of its volume  $V$  (m<sup>3</sup>) and inversely proportional to the distance  $d$  (m) from the source:

$$MA = \partial Jf(V)d^{-3}.$$

The magnetization contrast is composed of the difference between the two vectors, (i) induced magnetization  $J_i$  and (ii)  $J_r$ , where (i) is a product of  $\chi$  and the inducing local geomagnetic field  $H$  (A/m):

$$J = \chi H + J_r.$$

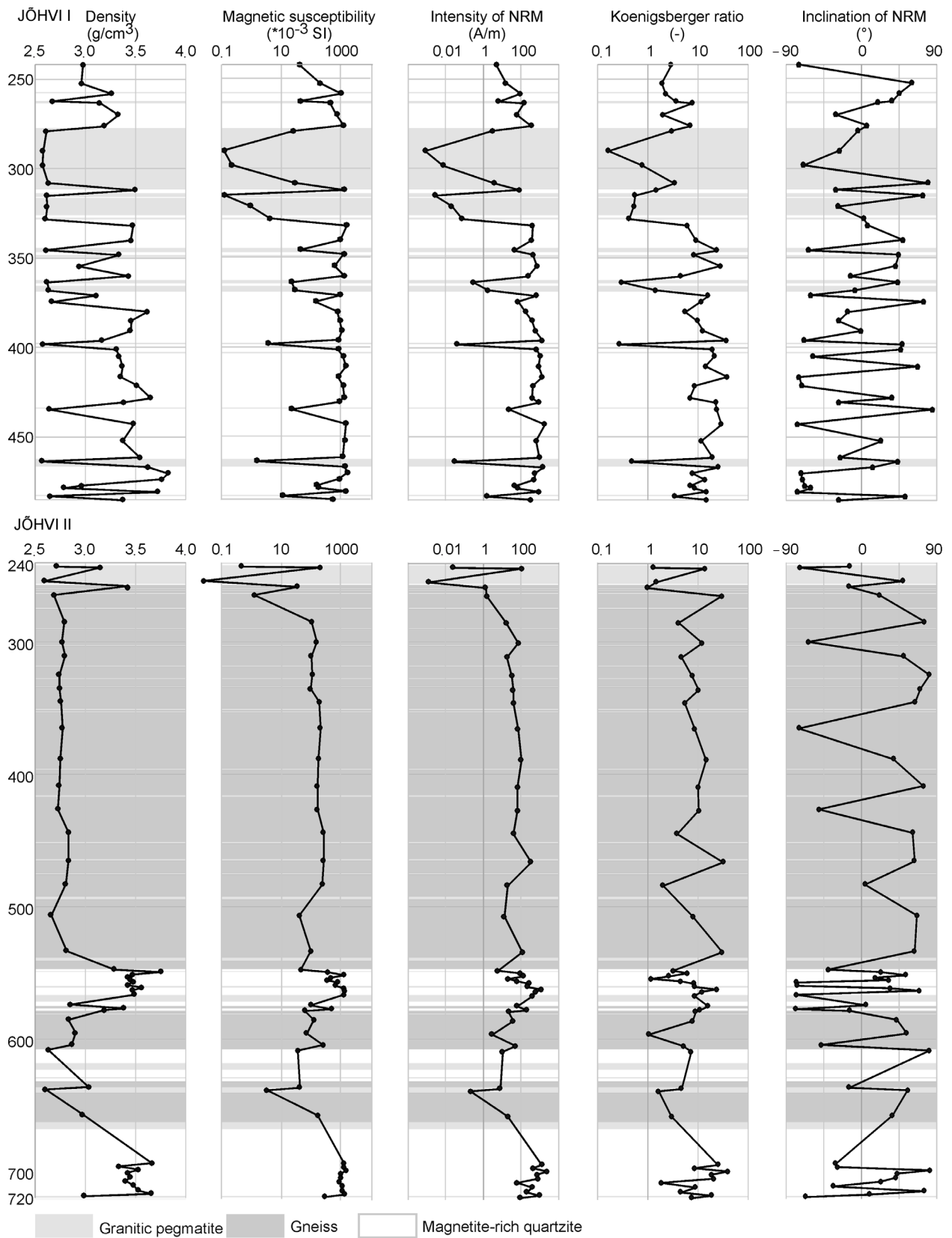


Fig. 2. Petrophysical properties of rocks in the Jöhvi I (above) and II (below) drill cores.

**Table 1.** Petrophysical properties (median, average and standard deviation) of Jõhvi core samples

Rock type	No.	Density (kg/m <sup>3</sup> )	Magnetic susceptibility ( $\times 10^{-3}$ SI)	NRM intensity (A/m)	Koenigsberger ratio (–)
<b>Jõhvi I core</b>					
Mt-quartzites	28	3406	1107	495.9	10.5
		3405 $\pm$ 197	1076 $\pm$ 300	597.9 $\pm$ 426.3	13.9 $\pm$ 10.1
Granitic pegmatite	15	2615	22	0.3	0.8
		2614 $\pm$ 32	24 $\pm$ 35	9.5 $\pm$ 19.0	4.8 $\pm$ 8.0
<b>Jõhvi II core</b>					
Mt-gneiss	26	3432	778	195.3	8.4
		3378 $\pm$ 247	691 $\pm$ 469	393.1 $\pm$ 522.6	11.0 $\pm$ 8.7
Granitic pegmatite	4	2644	1	0.1	1.5
		2648 $\pm$ 60	1 $\pm$ 1	0.4 $\pm$ 0.7	8.4 $\pm$ 14.0
Gneiss	20	2794	146	37.7	7.6
		2806 $\pm$ 87	140 $\pm$ 64	55.8 $\pm$ 68.3	9.1 $\pm$ 8.1

In the Jõhvi Mt-quartzites,  $J_r$  is the dominant part of the magnetization, with the proportion ( $Q$ ) between  $J_r$  and  $J_i$  being even  $>10$ . High  $Q$ -ratios, summarized by Puura et al. (1983) based on data from 30 drill cores and thousands of samples, characterize the Jõhvi structural zone in general (Table 2). Due to a large number of samples, variation in physical properties was large as well. For example, depending on the content of magnetite,  $\chi$  was found to vary between  $72 \times 10^{-3}$  and  $2124 \times 10^{-3}$  SI. In our models, however, we used magnetizations that are less than the averages for Mt-quartzite measured by ourselves (Fig. 2, Table 1) or by Puura et al. (1983). It is because our models theoretically consist of a mixture of Mt-quartzites with less magnetic varieties of gneisses. Assigning the modelled body values that respond to the measured ones would produce an unrealistically violent magnetic field.

Even the direction of  $J_r$  varies largely in the sample level. On a large scale it is directed normally, i.e. points

**Table 2.** Magnetic properties of the Jõhvi structural zone after Puura et al (1983)

Rock type	Magnetic susceptibility ( $\times 10^{-3}$ SI)	Koenigsberger ratio (–)
Migmatized metamorphic rocks in general	27.3	8.2
Migmatized metamorphic rocks excluding granitic interlayers	49.1	8.7
Granitic interlayers	1.6	3.0
Granitic gneisses	1.0	2.8
Biotite-amphibole-pyroxene gneisses	6.2	2.8
Alumogneisses	95.6	15.0
Mt-quartzite	747.8	11.1

downwards. This is the reason why the anomalies have a positive sign: if  $J_r$  was directed reversely, the anomalies would be negative. If  $J_r$  was directed towards a horizontal plane at angles  $<60^\circ$ , significant negative side anomalies would exist. Thus, during the modelling, among other variables,  $J_r$ , but especially  $I$ , had a specific role in controlling the shape and amplitude of response curves. Because of the absence of negative side anomalies in the Jõhvi area, the role of  $D$  in models was minor.

Strong  $J_r$  (high  $Q$ -ratio, Table 1) rules even over the shape of geometrical bodies used to simulate the measured field. For example, test usage of ellipsoids instead of elliptic cylinders provided similar results to the ones described above at the same petrophysical properties. The Potent software also allows tilting the cylinders and their top elliptic surfaces and calculating the response magnetic field, but the effect of tilting is minor compared to even slight changes in the direction of  $J_r$ . Thus, we decided to keep the axes of cylinders vertical and chose the most reasonable properties for  $J_r$  to characterize the source bodies.

The importance of high  $J_r$  in producing strong magnetic anomalies was first noted by Puura & Kuuspalu (1966) when they measured the physical properties of cores 315 and Jõhvi II. They note that, based on abundant studies of iron ores from the Ukrainian Kryvyi Roh Basin and Kursk magnetic anomaly (Krutihovskaya et al. 1964), the direction of  $J_r$  coincides with the dip of the formation. Our modelling supports this interpretation in Jõhvi as well. Strong values of  $J_r$  and high  $Q$ -ratios hint, however, at the contribution by the small ( $<1 \mu\text{m}$ ) grain size of magnetite (Dunlop 1973, 1990). Thus, partly not the quantity of magnetite but its quality is producing the Jõhvi anomalies. While decreasing the  $Q$ -ratio to 1 (virtually increasing the magnetite grain size) in the model of the western anomaly, the amplitude of the anomaly decreases to 4000 nT which is  $\sim 20\%$  of the present anomalous field

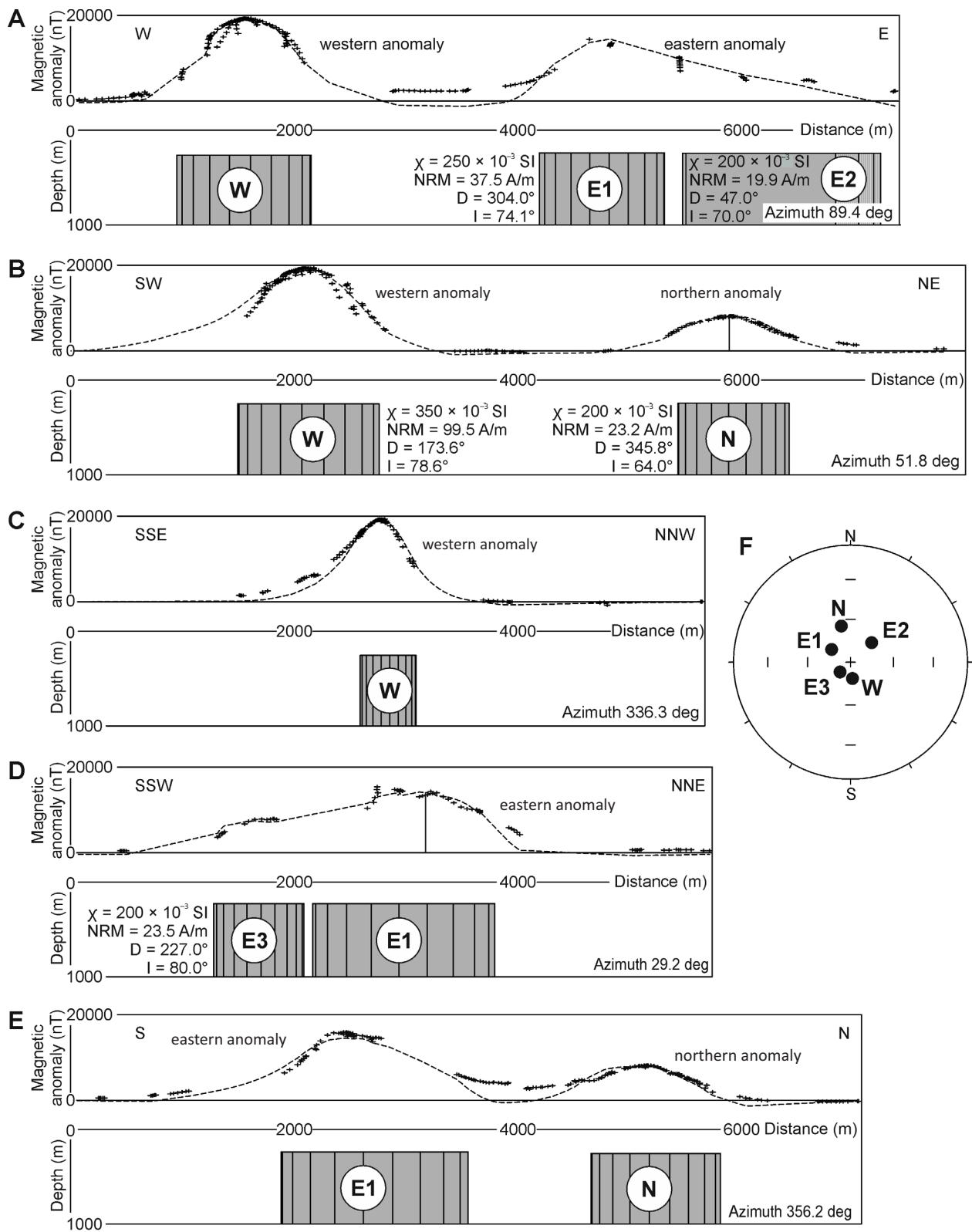


**Fig. 3.** A–E, cross sections of elliptic cylinders (E1, E2, E3, W, N and E, grey areas) along five profiles (see Figs 1B, 4 for location). The response curve is given (dashed line) and measured in the field original values (black + symbols). F, an equal area stereonet to illustrate the declination and inclination of natural remanent magnetization by individual cylinders. The vectors point downwards.

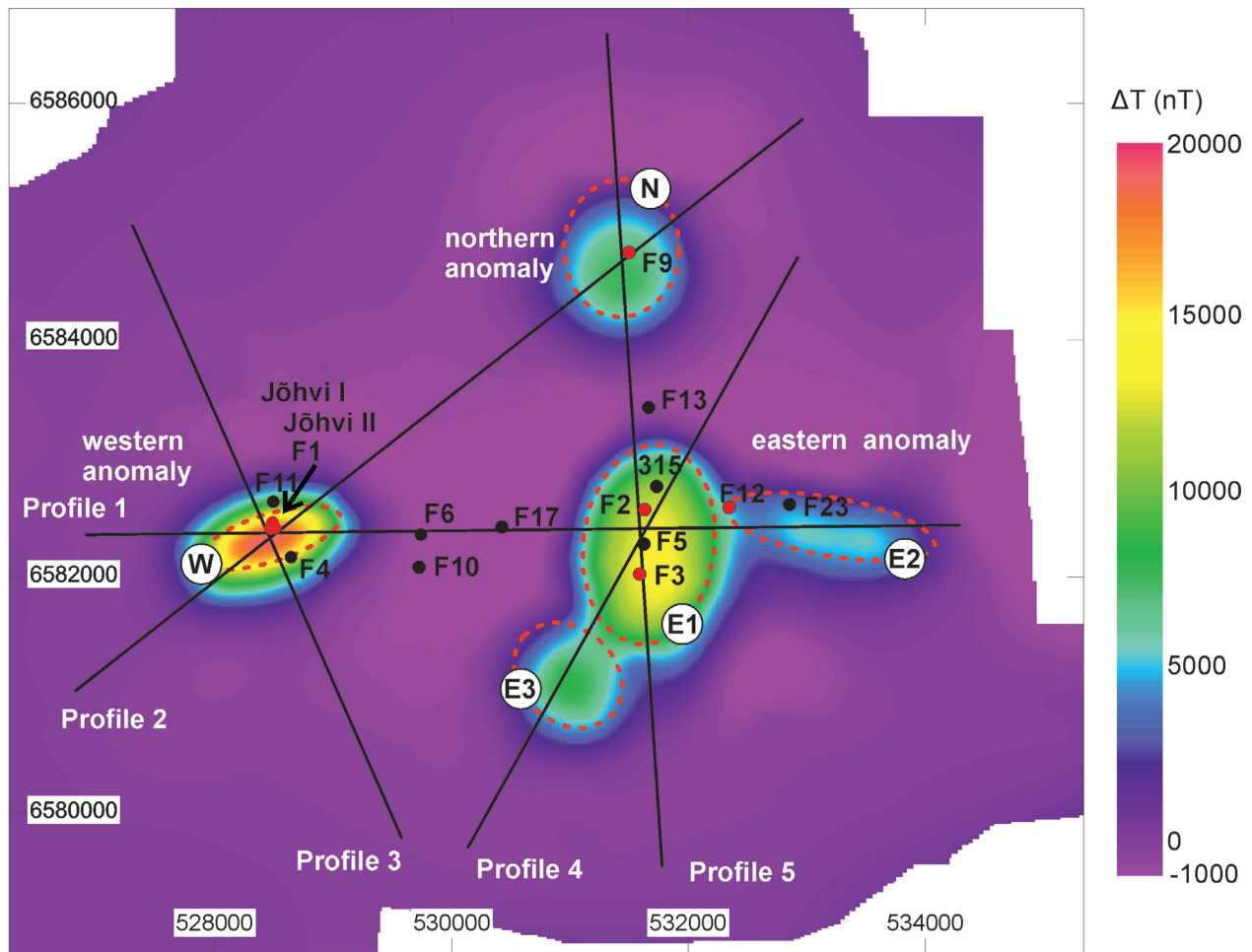


**Fig. 4.** Magnetic field calculated by five elliptic cylinders (red dashed lines) to simulate the Jõhvi anomaly by model. Shown are the profiles for the magnetic modelling and locations of drill holes. Red colour indicates the holes where Mt-gneiss has been discovered. Coordinates are in the UTM zone 35N.

only. To our best knowledge, no hysteresis of the Jõhvi ore has been studied to specify the content of the sub-micrometre magnetite.

Drilling has revealed a complex mixture of ore layers with granites, granitic pegmatites and gneisses, alternating from decimetres to tens of metres in width. Because the anomaly is inversely proportional to the distance from the source, and sizes of the individual source structures are magnitudes smaller than their depth, no complex details are seen in the measured magnetic field. Thus, the measured magnetic field expresses a lump sum of individual magnetic sources, whereas separation into signals of individual small-scale source structures is impossible due to the superposition principle.

The drilling activities in the 1960s resulted in five drill cores which opened the ore body (F1, F2, F3, F9, F12 in Fig. 4). Hole F1 was drilled side by side to the Jõhvi I and

II holes into the source of the western magnetic anomaly and opens Mt-quartzites in a depth of 234.2–443.0+ m. Drill holes F4 and F11 with depths of 271.25 and 297.6 m show the presence of magnetite on an accessory level only. Within the eastern anomaly, F2 and F12 have opened the ore body within a full length of the Proterozoic sequence (226.9–310.5 and 230.0–343.0 m, respectively). Drill core F3 opened a layer of Mt-gneiss at 230.0–254.5 m while the hole extended to 373.4 m. In F5, F23 and 315, only accessory magnetite was discovered. Three holes (F6, F10 and F17) within the area between the western and eastern anomalies opened granites and gneisses with accessory magnetite only. The holes were, however, short, opening 10–60 m of the crystalline basement. A similar presence of accessory magnetite was reported from F13 that opened the Precambrian basement at a depth of 219.3–267.6. A hole (F9) drilled into the northern anomaly opened an ore

body with interlayers of granites and gneisses within the full Palaeoproterozoic sequence at 228.0–305.8 m.

The FrEM experiment did not provide any new information on the shape and bedding of the western anomaly. It turned out that the frequency range used was too tight and the signal did not penetrate much below the Phanerozoic sediments. The signal was strong enough, but the lowest frequency (116 Hz) should have been even smaller. An example of the interpretation of one sounding is presented in Fig. 5 including a three-layer theoretical model. Considering the geological data from the Jõhvi F1 core (Fig. 1B; Erisalu et al. 1969), the layers correspond to (i) Quaternary glaciogenic sediments, Ordovician carbonate rocks and Lower Ordovician–upper Cambrian sandstones, (ii) Cambrian and Ediacaran clays and sandstones and (iii) crystalline basement. Most likely, the low electrical resistivity of the ~180 m thick pile of (ii) is

responsible for the failure of the method due to the screening of the primary electromagnetic field.

## CONCLUSIONS

The study provides a geological insight into the Jõhvi magnetic anomaly in NE Estonia. The investigation revealed that the three magnetic peaks with maximum amplitudes of 19 290 nT (western), 15 880 nT (eastern) and 8080 nT (northern) are caused mostly by strong remanent magnetization that is directed subvertically and pinpoints downwards. Petrophysical measurements of Mt-quartzites showed that the remanent magnetization surpassed the induced magnetization by about 10 times. Strong values of remanence hint at a significant contribution by the small (<1  $\mu\text{m}$ ) grain size of magnetite. Thus, partly, the small

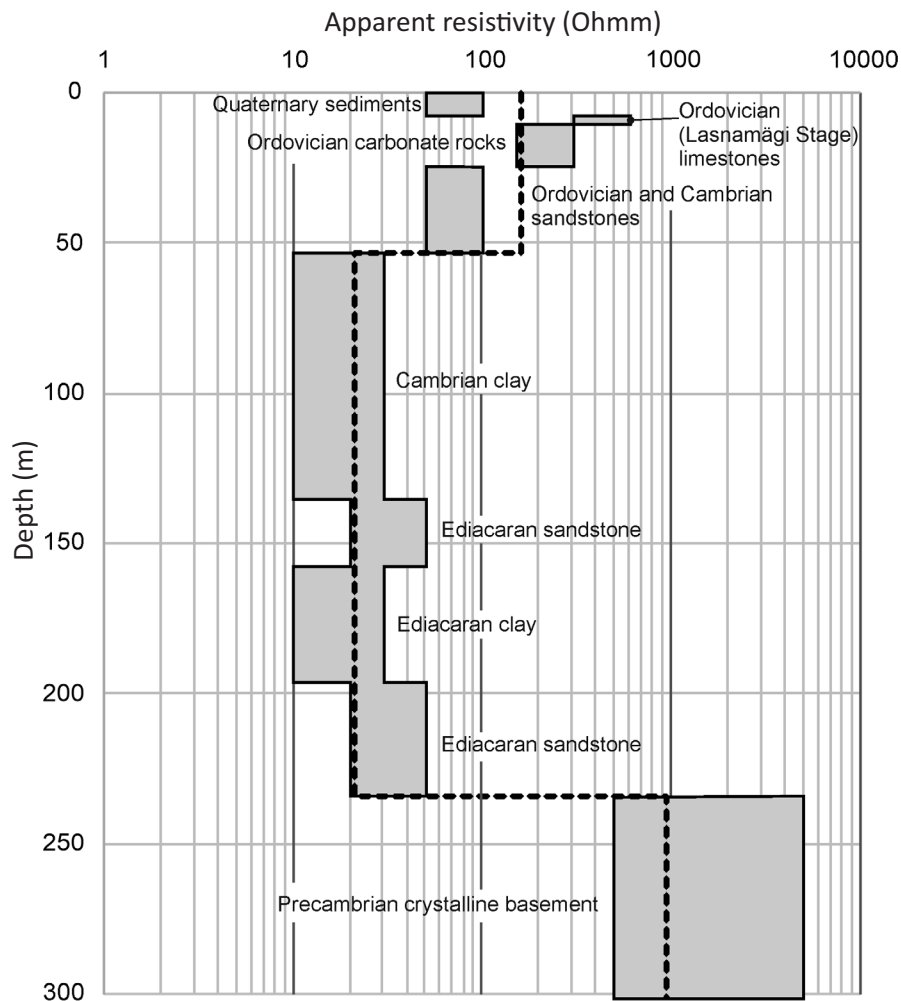


**Fig. 5.** Apparent electrical resistivity section at the Jõhvi western anomaly as based on the FrEM experiment. The grey areas mirror the geological section at the western anomaly (Erisalu et al. 1969) and apparent resistivities derived from Jõeleht & Kukkonen (2002).

grain size, not a huge volume of magnetite, is producing the outstanding Jõhvi magnetic anomalies.

**Acknowledgements.** We are grateful to Mikhail Shtokalenko and an anonymous reviewer for their constructive reviews. We thank Siim Ots for the preparation of samples and performing petrophysical measurements. Funding from the RITA programme by the European Regional Development Fund, the work programme 'Metallogenesis of the Jõhvi area' is acknowledged. The work by JP was supported by the Estonian Research Council project IUT20-34. The publication costs of this article were covered by the Estonian Academy of Sciences and the Estonian Environmental Investment Centre (project KIK17233).

## REFERENCES

- Aittoniemi, K., Rajala, J. & Sarvas, J. 1987. Interactive inversion algorithm and apparent resistivity versus depth (ARD) plot in multifrequency depth soundings. *Acta Polytechnica Scandinavica, Applied Physics Series*, **157**, 1–34.
- Bogdanova, S., Gorbachev, R., Skridlaite, G., Soesoo, A., Taran, L. & Kurlovich, D. 2015. Trans-Baltic Palaeoproterozoic correlations towards the reconstruction of supercontinent Columbia/Nuna. *Precambrian Research*, **259**, 5–33.
- Differt, E. D. 1936. *Magnetiit (magnetraua maak)* [Magnetite (Ore of Magnetic Iron)]. Ühiselu, Tallinn, 11 pp. [in Estonian].
- Dunlop, D. J. 1973. Thermoremanent magnetization in sub-microscopic magnetite. *Journal of Geophysical Research*, **78**, 7602–7613.
- Dunlop, D. J. 1990. Developments in rock magnetism. *Reports on Progress in Physics*, **53**, 707–792.
- Erisalu, E., Arvisto, E., Norman, A., Dantsenko, V., Koppelmaa, H., Niin, M. & Kivisilla, J. 1969. *Otchet po izuchenyu kristallicheskogo fundamenta Jyhviskoj magnitnoj anomalii i ee okrestnostej* [Report of the Basement Studies on Jõhvi Magnetic Anomaly and Nearby]. Geological Survey of Estonia, Kohtla-Järve, EGF 3032 [in Russian].
- Jõelet, A. & Kukkonen, I. T. 2002. Physical properties of Vendian to Devonian sedimentary rocks in Estonia. *GFF*, **124**, 65–72.
- Koistinen, T. (ed.). 1994. *Precambrian Basement of the Gulf of Finland and Surrounding Area, 1 : 1 mill.* Geological Survey of Finland, Espoo.
- Koistinen, T., Klein, V., Koppelmaa, H., Korsman, K., Lahtinen, R., Nironen, M., Puura, V., Saltykova, T., Tikhomirov, S. & Yanovskiy, A. 1996. Paleoproterozoic Svecofennian orogenic belt in the surroundings of the Gulf of Finland. *Geological Survey of Finland, Special Paper*, **21**, 21–57.
- Koppelmaa, H. (ed.). 2002. *Geological Map of the Crystalline Basement of Estonia. Scale 1 : 400 000.* Geological Survey of Estonia, Tallinn.
- Krutihovskaya, Z. A., Zavoiskij, V. N., Podolyanko, S. M. & Savenko, B. Ya. 1964. *Namagnichennost' porod zhelezorudnykh formatsii Bol'shogo Krivogo Roga i KMA* [Magnetization of Rocks from Iron Ore Formations from Great Krivoj Rog and Kursk Magnetic Anomaly]. Naukova dumka, Kiev, 179 pp. [in Russian].
- Linari, A. A. 1940. *Aruanne sügavpuurimistest Jõhvi lähedal* [Report on Diamond Drilling near Jõhvi]. Tallinna Tehnikaülikooli Toimetused, Ser. A, No. 15, 27 pp. [in Estonian, with English summary].
- Linhholm, A. A. 1937. Rakendus-geoloogilise oletusi Jõhvi magnetilise anomaalia piirkonna kohta [Magnetic anomaly of the district Jõhvi and its probable geological value]. *Tehnika Ajakiri*, **16**, 101–108 [in Estonian, with English summary].
- Melitskaya, V. I. & Papko, A. M. 1992. *Otchet o rezul'tatakh aeromagnitnoj s'emki masshtabov 1 : 25 000, 1 : 50 000 na territorii Õstonii i prilegayushchego shelfa, provedennoj partiei nr. 49 v 1987–1991 gg* [The Results of Aeromagnetic Mapping by Working Group No. 49 at Scales of 1 : 25 000 and 1 : 50 000 on the Estonian Territory 1987–1991. Report of Investigation]. Geological Survey of Belarus, Minsk, 75 pp. [in Russian].
- Nasuti, A., Roberts, D., Dumais, M.-A., Ofstad, F., Hyvönen, E., Stampolidis, A. & Rodionov, A. 2015. New high-resolution aeromagnetic and radiometric surveys in Finnmark and North Troms: linking anomaly patterns to bedrock geology and structure. *Norwegian Journal of Geology*, **95**, 217–244.
- Nehlig, P., Asfirane, F., Genna, A., Guerrot, C., Nicol, N., Salpeteur, I., Shanti, M. & Thiéblemont, D. 2002. Aeromagnetic map constrains cratonization of the Arabian Shield. *Terra Nova*, **13**, 347–353.
- Peters, L. J. 1949. The direct approach to magnetic interpretation and its practical application. *Geophysics*, **14**, 290–320.
- Pobul, E. 1961. *Seos magnetiliste struktuuride ja tektooniliste rikete vahel Eesti NSV põlevkivibasseini territooriumil (Jõhvi magnetiline anomaalia)* [Relationship Between Magnetic Structures and Tectonic Faults in the Territory of the Oil Shale basin in the Estonian SSR (Jõhvi Magnetic anomaly)]. Institute of Geology, Academy of Sciences of the Estonian SSR, Tallinn, EGF1604, 118 pp. [in Estonian, with Russian abstract].
- Puura, V. & Kuuspalu, T. 1966. *Metallogenicheskaya karta Õstonskoj SSR m-ba 1:500 000. Otchet III. Rudoproyavleniya v kristallicheskom fundamente uchastkov Yyhvi i Ul'yaste* [Map of Metallogeny of the Estonian S.S.R. in a Scale of 1 : 500 000. Volume III. Ore Occurrences in the Crystalline Basement of Jõhvi and Uljaste Areas]. Geological Survey of Estonia, Tallinn, EGF 2801, 267 pp. [in Russian].
- Puura, V., Vaher, R., Klein, V., Koppelmaa, H., Niin, M., Vanamb, V. & Kirs, J. 1983. *Kristallicheskij fundament Õstonii* [The Crystalline Basement of Estonian Territory]. Nauka, Moscow, 208 pp. [in Russian, with extended English summary].
- Rundqvist, D. V. & Mitrofanov, F. P. (eds). 1993. Precambrian geology of the USSR. *Developments in Precambrian Geology*, **9**, 1–527.
- Soesoo, A., Puura, V., Kirs, J., Petersell, V., Niin, M. & All, T. 2004. Outlines of the Precambrian basement of Estonia. *Proceedings of the Estonian Academy of Sciences, Geology*, **53**, 149–164.
- Soesoo, A., Kosler, J. & Kuldkepp, R. 2006. Age and geochemical constraints for partial melting of granulites in Estonia. *Mineralogy and Petrology*, **86**, 277–300.

- Soesoo, A., Nirgi, S. & Plado, J. 2020. The evolution of the Estonian Precambrian basement: geological, geophysical and geochronological constraints. *Transactions of the Karelian Research Centre of the Russian Academy of Sciences*, **2**, 18–33.
- Tikhomirov, S. N. 1966. *Geologicheskoe stroenie dokembrijskogo fundamenta v predelakh Leningradskoj oblasti i Pribaltiki* [*Geology of the Crystalline Basement in Leningrad Oblast and Baltics*]. VSEGEI, Leningrad, 24 pp. [in Russian].
- Vagapova-Kadyrova, M. D. 1948. *Dokembrijskie kristallicheskie porody i zhelezistye kvartsity Ėst. SSR* [*Precambrian Crystalline Rocks and Iron-Rich Quartzites of the Estonian S.S.R.*]. Ministry of Geology of the S.S.S.R., Leningrad, 228 pp. [in Russian].

## Jõhvi rauamaagi magnetanomaalia, kontrollitud subvertikaalse jääkmagnetiseerituse poolt

Jüri Plado, Kalle Kiik, Jarkko Jokinen ja Alvar Soesoo

Jõhvi magnetanomaalia paikneb Kirde-Eestis Jõhvi struktuurse vööndi piires. 1930. ja 1960. aastatel läbiviidud puurimiste tulemusel avastati piirkonna aluskorrast graniitide, pegmatiitide ning gneissidega vaheldumisi rauamaaki. Käesoleva uuringu käigus viidi läbi piirkonna täpsustav maapealne magnetomeetriline kaardistamine ja elektromagnetilised (FrEM) mõõtmised, mõõdeti Jõhvi I ja II puursüdamiku füüsikalisi omadusi (tihedus, magnetiline vastuvõtlikkus, jääkmagnetiseerituse intensiivsus ja inklinatsioon) ning modelleeriti anomaaliaid põhjustavad struktuurid. Magnetanomaalia koosneb kolmest osast, mille maksimaalsed amplituudid on 19 290 nT (läänepoolne), 15 880 nT (idapoolne) ja 8080 nT (põhjapoolne). Anomaaliaid põhjustavaid kehasid modelleeriti elliptiliste silindrite abil, millel on vastavalt raua sisaldavate kivimite füüsikaliste omaduste mõõtmisele tugev jääkmagnetiseeritus. Viimane on suunatud maa sisemuse poole subvertikaalselt, st kallutatusega, mis sarnaneb puursüdamikes määratud kihtide kallutatusele. Maagi tugev jääkmagnetiseeritus viitab pisikeste (<1 µm) magnetiiditerade esinemisele. Elektromagnetiliste mõõtmiste käigus ei õnnestunud väikese takistusega Kambriumi ja Ediacara savide ning liivakivide ekraniseeriva mõju tõttu maagikehade lasumuselemente täpsustada. Samas kattusid uuringutulemused meie varasemate teadmistega Jõhvi geoloogilise läbilõike elektriliste takistuste kohta.